Fluctuators in disordered metallic point contacts: a simulation approach

1998 J. Phys.: Condens. Matter 10 8033

(http://iopscience.iop.org/0953-8984/10/36/013)

J. Phys.: Condens. Matter **10** (1998) 8033–8047. Printed in the UK PII: S0953-8984(98)92209-3

Fluctuators in disordered metallic point contacts: a simulation approach

V I Kozub† and C Oligschleger‡

Institut für Festkörperforschung, Forschungszentrum Jülich, D-52425 Jülich, Germany

Received 3 March 1998, in final form 17 June 1998

Abstract. Electron transport through amorphous monatomic metallic structures generated earlier by molecular dynamics simulations is studied numerically. The interference of electronic trajectories backscattered by the structural disorder probes the multistable structural relaxations responsible for low-frequency noise in real metallic contacts. The structure of these modes is illustrated; the dependence of the magnitude of the noise on the size and structure of the modes is studied. The transition from a multistable behaviour to a more complex one is observed for temperatures far below the melting temperature. The current fluctuations observed numerically resemble the complex behaviour reported earlier for current noise in small metallic structures at moderate temperatures.

1. Introduction

In recent years substantial progress in the study of the flicker noise problem was achieved. This is mainly connected with experiments on small conducting systems, where the $1/f$ noise was decomposed [1, 2] into a sum of contributions due to 'elementary' defects with internal degrees of freedom—'fluctuators'. These defects switch between two possible configurations and cause the 'telegraph' resistance noise in small contacts. In metallic systems they are believed to be related to structural defects which at low temperatures are seen as the well-known two-level systems [3–8]. We would also like to mention work where the two-level fluctuation studied exists in atomic-size contacts produced with the help of the break-junction method [9]. However, there is still no clear understanding of the microscopic nature of these defects.

Many experimental results can be explained [10] by the model of independent fluctuators described by rate equations for the occupation numbers. The soft-potential approach which relates the fluctuators to certain 'soft' double-well effective potentials has been used to describe this picture [8, 10]. It fails, however, to give a microscopic insight into the problem. On the other hand, some experiments revealed a much more complex behaviour, exhibiting in particular fluctuator interactions and non-stationary chaotic behaviour of the fluctuator parameters [2]. These features cannot easily be described within the framework of the soft-potential model. Thus a microscopic analysis of the problem would be desirable. However, a description of disordered materials based on purely analytical methods encounters obvious

† Permanent address: A F Ioffe Physico-Technical Institute, 194021 St Petersburg, Russia.
‡ Present address: Institut für Physikalische und Theoretische Chemie, Universität Bonn, D-53115 Bonn, and Institut für Algorithmen und Wissenschaftliches Rechnen, GMD—Forschungszentrum Informationstechnik, D-53754 Sankt Augustin, Germany.

0953-8984/98/368033+15$19.50

difficulties. Numerical simulations based on molecular dynamics (MD) methods are used successfully to model the structure of glassy materials as well as their thermodynamic properties including the density of states. In particular, many details related to low-energy vibrational excitations in these materials have been revealed in this way [11]. To our knowledge, electron transport through disordered media has not been treated by these numerical methods.

Real metallic point contacts studied experimentally can be as small as 3–10 nm in diameter and thus consist of only $\sim 10^3$–10^4 atoms, which is just of the order accessible to numerical simulations. Moreover, the structure of these constrictions is not expected to be perfectly crystalline especially in view of the amorphous films used to prepare these point contacts.

Therefore, it is attractive to use a simulation approach to study slowly relaxing metastable configurations in disordered metallic structures with an application to low-frequency noise. In the following we will give the results of a first such study of noise within the framework of simplified model considerations.

The main results of our paper described in the following are:

(1) We have identified local atomic arrangements leading to metastable configurations.

(2) A transition from a simple telegraph signal to a more complex behaviour with increasing temperature was observed which reproduces the experimental behaviour; it is important that the ratio of this 'critical' temperature to the melting temperature agrees with experiment.

(3) The magnitude of the resistance fluctuations and its dependence on the number of atoms forming the 'fluctuator' is considered; the results of the simulations are in agreement with experiment.

2. Theoretical aspects

Our aim is to analyse numerically charge transport through disordered structures prepared previously by molecular dynamics [12]. The structures studied are considered to model 3D cubic microbridges (with side length a) between bulk contacts. The atoms forming the structures are taken to be scatterers for the incident electrons. We consider the weak-scattering limit where the mean free path of the electrons, l, is larger than a. This implies that the scattering cross-section s obeys the inequality $n_i s < a^{-1}$ where $n_i = N/a^3$ and N is the total number of atoms in the structure. In real glassy metals the mean free path is significantly larger than the electron wavelengths, and, therefore, the approximation is justified for nanoscale point contacts.

To study the conductance changes caused by 'jumps' in the structural configurations we relate them to the changes of the interference contribution to the backscattered electron flux in the contact region. The weak-scattering approximation allows us to neglect multiple scattering, restricting our calculations to a minimal number of scattering events. This corresponds to the concept of local interference which has been introduced in reference [13] for the case of scattering by complex defects [14]. Mesoscopic effects in bulk samples caused by local interference of a more general type have been considered in reference [15].

The standard approach to the conductance G of small contacts exploits the Landauer formula (see, e.g., reference [16])

$$G = \frac{e^2}{h} \sum_{\alpha} (1 - R_\alpha) \tag{1}$$

where R_α is the reflection coefficient for channel (mode) α. In a simulation, one needs to identify these modes α. This can easily be done for 2D quantum point contacts with smooth 'adiabatic' boundaries [17], whereas for realistic structures one meets with considerable problems. In particular we mention reference [18] where for the case of a short 2D channel the conductance is calculated numerically by matching the 'bulk' plane-wave modes to the channel's transversal modes.

Here, we will apply the 'wave optics' approach which was developed for the transport in structures with a small number of scattering events and is in the spirit of reference [18]. In reference [19] this approach was developed and successfully applied to analyse experimental data on mesoscopic transport in 3D ballistic point contacts with diffusive surroundings. We also want to mention the simulations of quasi-ballistic transport in static disordered structures [20] based on the Green's function method whose results agree well with those of reference [19].

The 'wave optics' approach exploits the fact that for metallic point contacts transport is always semiclassical in the sense that the number of quantum channels is large, corresponding to the 'geometrical optics' approximation for the de Broglie waves. For an ideal point contact, separating the bulk leads, the modes α correspond to the 'optical beams' cut by the orifice from the incident plane waves $\boldsymbol{k}$. The 'quantization' of the modes originates from the Fourier expansion of the kernel of the Fresnel–Kirchhoff integral which describes the diffraction of the incident plane wave by the aperture in an opaque screen; see, e.g., reference [21]. The number of the modes, $\sim(k_F a)^2$ (with $\boldsymbol{k}_F$ the Fermi wave vector), is the number of independent solutions of the diffraction problem for a given $|\boldsymbol{k}| \approx k_F$.

To calculate the backscattering coefficients R_α within this approach we use the standard perturbation theory of scattering using Schrödinger's equation [22]. We consider the scattering of the incoming modes ψ_α which, as discussed above, at distances of the order of the atomic scale, can be approximated by plane waves with wave vectors $\boldsymbol{k}_\alpha$. The resulting wave, scattered by a scatterer i at point $\boldsymbol{R}_i$, is

$$\psi_{s,\alpha}(i,\boldsymbol{r}) = \frac{\psi_\alpha(\boldsymbol{R}_i)F_i}{|\boldsymbol{r}-\boldsymbol{R}_i|}\exp(\mathrm{i}k|\boldsymbol{r}-\boldsymbol{R}_i|)). \tag{2}$$

Here F_i is the scattering amplitude which in the following we assume to be equal for all scatterers ($F = (s/4\pi)^{1/2}$). Including multiple scattering would add higher-order terms in F/a. For a random distribution of scatterers the sum over all possible configurations would give a factor $\sim N^{1/2}$ to the correction of the wave-function equation, expression (2). Thus the total contribution of trajectories involving multiple scattering is via a factor

$$s^{1/2}N^{1/2}/(a(4\pi)^{1/2}) = s^{1/2}n_i^{1/2}a^{1/2}/(4\pi)^{1/2} \ll 1$$

which is smaller than the contribution due to single scattering, i.e. neglecting multiple scattering is justified.

The coefficient R_α is by definition the ratio of the 'backscattered' current to the 'incident' current of the mode α. In our approximation we have

$$R_\alpha = \frac{1}{v_{\perp,\alpha}|\psi_\alpha|^2}\int_S \mathrm{d}^2\boldsymbol{r}\ \frac{\mathrm{i}e\bar{h}}{2m}(\langle\psi^*_{s,\alpha}|\boldsymbol{\nabla}|\psi_{s,\alpha}\rangle + \mathrm{CC}). \tag{3}$$

Here $\psi_{s,\alpha}$ is the sum of the waves scattered by the scatterers i and $v_{\perp,\alpha}$ is the velocity of the incident electron wave perpendicular to the aperture. The apparent divergency due to $v_{\perp,\alpha}$ in equation (3) is integrable since $v_{\perp,\alpha} \propto (k_F - k_{\alpha,\perp})^{1/2}$, with $\boldsymbol{k}_{\alpha,\perp}$ the projection of $\boldsymbol{k}_\alpha$ onto the orifice plane, and does not affect the final result of equation (4). S is the orifice area while $\boldsymbol{r}$ is the 2D radius vector in the detector plane. Figure 1 depicts schematically two backscattered trajectories which interfere in the detector plane.

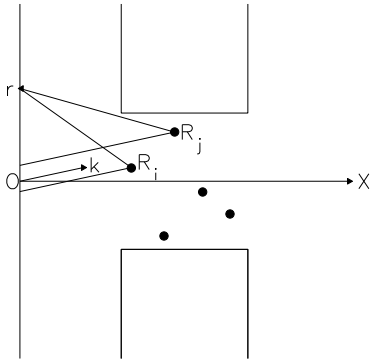

Figure 1. A schematic plot of backscattered trajectories each involving one atom acting as a scatterer of the incident electron wave. The incident wave is represented by its wave vector $\boldsymbol{k}$. Filled circles depict some of the atoms in the point contact. R_i and R_j denote the positions of the atoms and r the two-dimensional radius vector in the detector plane.

From equations (2) and (3) we get for the change of the conductance due to backscattering

$$W_b \equiv \frac{\delta G_b}{G} = \left(F^2 \Big/ \sum_\alpha (1 - R_\alpha) \right) \times \sum_\alpha \int_S \mathrm{d}^2 \boldsymbol{r} \sum_{i,j} \frac{\cos(k_F(|\boldsymbol{r} - \boldsymbol{R}_i| - |\boldsymbol{r} - \boldsymbol{R}_j|) + \boldsymbol{k}_\alpha \cdot (\boldsymbol{R}_i - \boldsymbol{R}_j))}{|\boldsymbol{r} - \boldsymbol{R}_i||\boldsymbol{r} - \boldsymbol{R}_j|} \times (\cos(\angle(\mathrm{O}X, \boldsymbol{r} - \boldsymbol{R}_i)) + \cos(\angle(\mathrm{O}X, \boldsymbol{r} - \boldsymbol{R}_j))). \quad (4)$$

Here OX is the contact axis. Equation (4) is the basic input for the numerical studies described below. The advantage of the coordinate representation used in our approach is its direct contact with the simulation of electron transport through the structure. In our calculations we consider amorphous structures where all atoms act as scatterers. For relatively clean crystalline structures only defect atoms are responsible for backscattering. We are mainly interested in the changes of the backscattering due to changes of the structures and use all atomic positions as input for equation (4). In the absence of defects one would obtain the conductance of purely ballistic contact from the Landauer formula, equation (1).

3. Computational details and results

With the help of equation (4) we carried out numerical studies of the backscattered current for amorphous and crystalline monatomic metallic structures and for amorphous selenium. We would like to note, however, that dealing with monatomic metallic glasses one meets difficulties due to their strong tendency to crystallize. This problem is known both from experiments on real metallic glasses and from computer simulations. One consequence is that the structural relaxations are mostly irreversible, preventing the formation of multistable structures supposed to give rise to the 'fluctuators'. We will discuss these problems in more detail in relation to the results of our simulations. Additionally we have calculated the backscattered electron flux by using a more complex structure of amorphous Se, which is much more stable against crystallization. The results of the MD simulation [23, 24] have shown that both soft-sphere and Se glasses behave similarly as regards their dynamics,

which for both systems at low temperature exhibits local relaxations. Although electron transport in real Se-based structures is hardly similar to that in metals, we believe that the simulations for the corresponding model structures are in any case instructive. Indeed, one should keep in mind that 'fluctuators' are thought to be related to defect regions where the structure might be even more complex than in a monatomic metallic glass.

The metallic structures were generated in earlier MD simulations [11, 12, 24]. The interatomic interaction in these systems is given by a soft-sphere potential

$$V(r) = \epsilon(\sigma/r)^6 + A(r/\sigma)^4 + B$$

where the energy scale is given in units of ϵ and the length scale in units of σ. In the simulations we used the units $\epsilon = \sigma = m = 1$, m being the atomic mass. The density is kept constant at $\rho\sigma^3 = 1$ and the nearest-neighbour distance corresponds to about 1.1σ. To reduce the numerical effort, the potential is cut off at $r_c/\sigma = 3.0$ and shifted by a polynomial $A(r/\sigma)^4 + B$ with $A = 2.54 \times 10^{-5}\epsilon$ and $B = -3.43 \times 10^{-3}\epsilon$. Both the potential and the force are zero at the cut-off. Such a potential is appropriate to model metallic systems [25].

As described by Laird and Schober [11], to bypass crystallization the model glassy structures were produced from well equilibrated liquids by a rapid quench. With typical quench rates of the order $0.25k_B/\sqrt{m\sigma^2/\epsilon}$ the configurations are cooled to roughly half the glass-transition temperature T_g and left there for more than 1200 molecular dynamics time-steps (MDS), i.e. about 60 typical vibration periods, to stabilize the potential energy. The local minima of the structures were found by minimizing the potential energy with a steepest-descent/conjugate-gradient algorithm [26]. To obtain a reasonable statistics for the structures consisting of 500 and 1024 atoms, in all 60 and 21 model glassy structures were produced, respectively.

The structural changes of these metallic glasses were observed in a previous molecular dynamics simulation [12]. To study the dynamics of these soft-sphere glasses they were heated with help of the 'Velocity–Verlet' algorithm in stages to temperatures ranging from $0.05T_g$ to $0.125T_g$. The molecular dynamics simulation was carried out with periodic boundary conditions to reduce surface effects. After heating the glasses to the desired temperature, the temperature was kept constant by scaling the velocities of the atoms. At each temperature the dynamics of the systems was followed for 9000 time-steps, which corresponds roughly to 500 periods of a typical vibration.

To observe more complex structures and to reduce further the 'finite-size' effects, additionally 15 soft-sphere glasses with $N = 5488$ were generated from hot melts and used to study relaxations in a greater detail [24]. These glasses were heated to temperatures ranging from $0.05T_g$ up to $0.15T_g$ and left there for 90 000 MDS (an order of magnitude longer than for the smaller systems).

During the molecular dynamics simulations at constant temperature the configurations move to new minima of the energy landscape due to processes of local hopping over small energy barriers. To detect new configurations on the energy hypersurface the displacements of the atoms from the metastable equilibrium positions $\boldsymbol{R}_n^i$ of atom n in configuration i are measured and the total displacement of the structure is defined as

$$\Delta R^2(t) = \sum_n (\boldsymbol{R}_n(t) - \boldsymbol{R}_n^i)^2 \tag{5}$$

where $\boldsymbol{R}_n(t)$ is the actual position vector of atom n. If the total displacement of the atoms exceeds a cut-off value and the residence time of the atoms in the new positions also exceeds a minimal period of at least three soft, low-frequency vibrations (several hundred MDS) the new positions of the particles are accepted as a new minimum configuration. The cut-offs

of the displacement and residence time, respectively, are chosen such that spurious minima are avoided. This procedure is described in greater detail in references [12, 24].

These minima are monitored during the molecular dynamics runs. The corresponding relaxations from one minimum to another can be either reversible or irreversible. The irreversible jumps are mainly due to the instability of the monatomic metallic glasses. This instability manifests itself in the fact that during the observation time some of the samples partially crystallized. Such a crystallization is connected with a global rearrangement of nearly all atoms in the configuration. This effect depends strongly on the size of the samples used in the simulation. The larger the system, the more stable the configurations. The largest systems show greater stability towards crystallization; just one configuration (out of 15 with $N = 5488$ atoms) crystallized during the observation time at a temperature $T = 0.15T_g$. But the tendency to lower the potential energy persists during the simulation.

Therefore, the first jumps after heating up to different temperatures are related to non-local rearrangements of the glasses, i.e. jumps with large displacements involving many atoms and leading to more stable configurations. These jumps are followed by relaxations located at only a few atoms. A measure for the localization of a jump is the effective mass

$$M_{\text{eff}} = m\frac{(\Delta R)^2}{|\Delta \boldsymbol{R}_{\max}^2|} \tag{6}$$

where

$$(\Delta R)^2 = \sum_n (\boldsymbol{R}_n^i - \boldsymbol{R}_n^f)^2$$

is the square of the total distance ΔR between two successive minimum configurations (called 'initial' and 'final' positions of the jump). $\boldsymbol{R}_n^{i,f}$ denotes the respective initial and final positions of atom n; $|\Delta \boldsymbol{R}_{\max}^2|$ is the maximal distance that a single atom jumps in this relaxation. Since we take the masses of the atoms comprising the structures as equal, M_{eff} counts the effective number of particles contributing to the hopping process.

In an extended computer simulation it is found that the displacement of a single atom in the relaxation is only a fraction of the nearest-neighbour distance (typically a tenth of a bond length), i.e. relaxations at low temperatures are local processes with small displacements of the atoms contributing to this thermally activated jump. However, even the small displacements of the single activated atoms exceed the vibration amplitudes. Since the typical total distance between two minimum configurations is about one or several nearest-neighbour distances [27], the effective mass is of the order of 10 to 100 atoms contributing essentially to the relaxations. It is found that these entities of some ten particles involved in the hopping processes form chain-like structures which move collectively along these chains [28].

Since we are interested in multistable configurations, we restrict ourselves to the relatively rare reversible changes of the configurations, which means that the initial configuration and the final one of successive jumps are identical. A measure for the reversibility of successive jumps can be given by the quantity $c_{RR'}$:

$$c_{RR'} = \frac{1}{\Delta R\,\Delta R'}\sum_{n=1}^{N} |\Delta \boldsymbol{R}_n||\Delta \boldsymbol{R}'_n| \tag{7}$$

where $\Delta \boldsymbol{R}_n = (\boldsymbol{R}_n^i - \boldsymbol{R}_n^f)$ is the displacement vector of atom n in the relaxation ΔR ($\boldsymbol{R}_n^{i,f}$ being, as above, the initial and the final positions of atom n in the relaxation ΔR), and ΔR

and $\Delta R'$ are the total jump lengths of two successive relaxations, given by

$$\Delta R^2 = \sum_{n=1}^{N} (\Delta \boldsymbol{R}_n^2).$$

For a reversible jump one has $c_{RR'} = 1$, i.e. the same atoms are contributing equally to the two jumps. If the jumps were uncorrelated, $c_{RR'}$ would be of the order of $c_{RR'} = N_p/N$, where N_p is the number of atoms involved in the hopping. During the MD runs of the 60 glasses with 500 atoms only two structures undergo reversible jumps, whereas for the glasses with 1024 soft spheres only one reversible relaxation occurred. The effective masses of the reversible relaxations observed in soft-sphere glasses with $N = 500$ and 1024 atoms range from 6 to 16 atomic masses. At $T \approx 0.1T_g$, half of the glasses with $N = 5488$ settled during the observation time to configurations where reversible jumps involving up to four local minima are observed. For the simulations with 5488 atoms, reversible relaxations with effective masses from 9 to 50 atoms were found.

In order to calculate the electron backflow we use incident electron waves with $\boldsymbol{k}$-vectors of length $k = \pi/\sigma$. This value determines the 'discretization' of the numerical integration in equation (4). The summation over the modes in equation (4) becomes a sum over discrete angles which we take as $\Delta\phi = 2\pi/ka$ and $\Delta\theta = \pi/ka$, where a is the side length of the amorphous sample; for the metallic glasses the side length is $a = N^{1/3}\sigma$. Using different grids for the numerical discretization changes the results by only a few per cent, i.e. they are not crucially sensitive to the specification of the modes. To escape numerical problems with vanishing denominators in equation (4) we integrated over r not in the front orifice plane but instead in a 'detector' plane shifted by approximately one atomic distance from the orifice plane. The integration becomes a double sum with $x = i\,\Delta x$ and $y = j\,\Delta y$ where $\Delta x = \Delta y = 1/k$. The detector plane is taken about two to three times larger than the orifice; the thus-neglected backscattered current is less than 10–25%. As the value of the scattering amplitude F, we take (typical for metals) $k_F F \simeq 1$. One can show that for a relatively small contact volume (small a and N) the weak-scattering approximation ($sN/a^2 < 1$) holds with this assumption.

To test our procedure we applied it to the simple case of a self-interstitial atom in an fcc metal. This so-called dumb-bell configuration is formed by replacing one atom by a pair of atoms aligned in the (100) direction [29]. The elementary jump process of this self-interstitial atom configuration is to a nearest-neighbour site and involves a change of orientation to a different cubic axis, i.e. the dumb-bell is now aligned in a (010) or (001) direction. Using the soft-sphere potential we construct configurations comprising 501 atoms with the dumb-bell in the middle of the structure aligned in (100) and (001) directions. The coordinates of the atoms are then used as input for equation (4) to calculate the backscattering of these structures. For the configuration with the dumb-bell in the (100) direction, i.e. perpendicular to the detector plane (see figure 1), we find $W_b = 0.536$, and for the two other orientations, (001) and equivalently the (010) alignment, parallel to the detector plane, we calculate $W_b = 0.540$. From this we deduce that the relative magnitude of the fluctuation due to the reorientation of the dumb-bell is about 0.7%.

In the following we present the relative magnitudes of the fluctuations caused by jumps and relaxations in monatomic metallic glasses and defect structures as described above. Since we are interested in the changes of the backscattered flow due to relaxations of the samples, we determine the minima observed in the MD runs and calculate W_b for these structures corresponding to the local minima of the potential energy. We neglect the contribution of atomic vibrations to the electronic backscattering, which will be similar for different configurations.

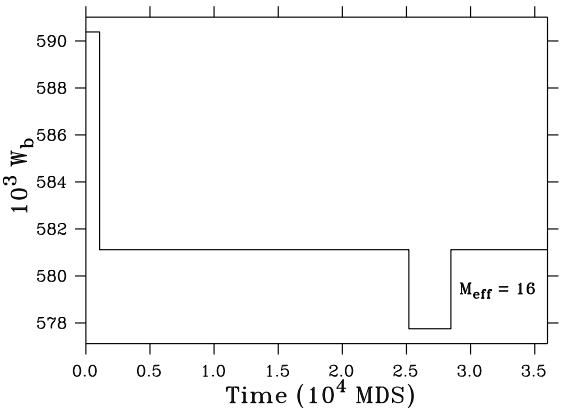

Figure 2. The fluctuator behaviour of a configuration with $N = 500$ atoms. W_b is plotted against time in units of MDS. The reversible relaxation at $t \approx 25\,000$ MDS has an effective mass $M_{\text{eff}} = 16m$ and a total jump length $\Delta R = 1.03\sigma$.

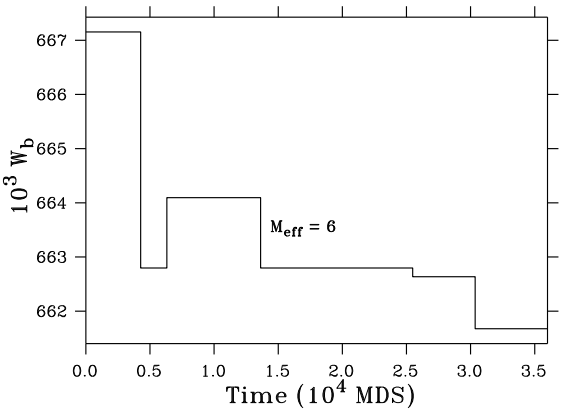

Figure 3. The fluctuator behaviour of a configuration with $N = 1024$ atoms. W_b is plotted against time in units of MDS. The reversible relaxation at $t \approx 6000$ MDS has an effective mass $M_{\text{eff}} = 6m$ and a total jump length $\Delta R = 0.44\sigma$.

In figure 2 we show W_b for a metallic glass with $N = 500$ atoms. After the initial rearrangement connected with a decrease in potential energy, the system was stable for more than 20 000 MDS before a reversible jump occurred with a total jump length of $\Delta R = 1.03\sigma$ and an effective mass $M_{\text{eff}} = 16m$. The relative magnitude of the backscattered current is about 0.6%.

Figure 3 shows W_b for a system with $N = 1024$ atoms. After approximately 6000 time-steps a reversible jump occurred with a total jump length of $\Delta R = 0.44\sigma$ and an effective mass $M_{\text{eff}} = 6m$. The fluctuation due to the structural relaxation is approximately 0.2% of the total interference contribution.

To simulate more complex multistable atomic aggregates, larger samples are needed. Indeed, as we have discussed, the smaller systems are relatively unstable, thus preventing extended multistable atomic aggregates from forming. Therefore, we have also studied the current transport based on the results for a glass with $N = 5488$ atoms. To shorten simulations of the interference pattern we restricted the summations over the scattering

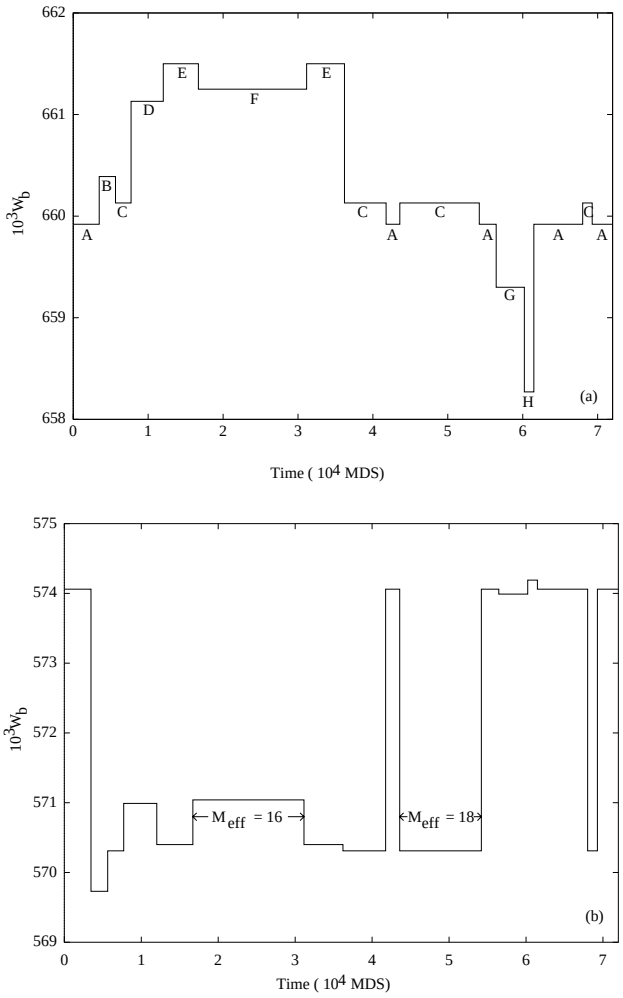

Figure 4. The fluctuator behaviour in a glass of 5488 soft spheres undergoing fifteen jumps between eight minima denoted by A, B, C, ..., H. Different directions of detector planes are shown: (a) plane $\perp$ x-axis and (b) plane $\perp$ z-axis. Two direct reversible relaxations (with effective masses $M_{\rm eff} = 16m$ and $M_{\rm eff} = 18m$ and corresponding jump lengths $\Delta R = 0.72\sigma$ and $\Delta R = 1.22\sigma$) can be observed. W_b is plotted against time in units of MDS.

atoms R in equation (4) to a subset $N_s \approx 700$ of the atoms including and surrounding the active ones.

The conductance change of this glass heated to $0.1T_g$ and aged for 90 000 MDS is shown in figure 4. In figure 4(a) we show the signal of the backscattering for the detector placed perpendicular to the arbitrarily chosen x-axis of the structure, while in figure 4(b) we measure the backscattered current in the plane perpendicular to the z-axis of the point contact, i.e. we have placed the detector parallel to the xy-plane of the sample of the configuration and the bulk leads are now perpendicular to the xy-plane of the nanoscale point contact. The results of the backscattering are much more complex than the ones described above for the smaller systems: the complex behaviour of the conductance change shown in figure 4 results from 15 jumps between eight minima denoted by A, B, C, ...,

H according to their occurrence during the simulation. After an initial drop in energy the glass relaxes to a (meta)stable region in the configurational space, where we monitored these strongly correlated jumps between eight minima of nearly equal energy. After about 17 000 MDS a reversible jump (E $\rightarrow$ F $\rightarrow$ E) occurred with a total jump length $\Delta R = 0.72\sigma$ and an effective mass $M_{\rm eff} = 16m$. At $t \approx 42\,000$ MDS the glass returns to minimum A and relaxes to minimum C ($\Delta R = 1.22\sigma$ and $M_{\rm eff} = 18m$) and again back to minimum A. After visiting two other minima G and H, the jump pattern (A $\rightarrow$ C $\rightarrow$ A) is repeated.

The magnitude of the relative backscattered electron flux is about 0.037% for the contribution of the first reversible relaxation (E $\rightarrow$ F $\rightarrow$ E) measured in a detector plane perpendicular to the x-axis of the sample (see the experimental set-up in figure 1) and 0.032% for the second pronounced fluctuation (A $\rightarrow$ C $\rightarrow$ A).

The signal of these fluctuators changes drastically when we measure the backscattered current in the plane perpendicular to the z-axis of the configuration. As described above, we have placed the detector parallel to the xy-plane of the sample. The change of the experimental set-up enables us to detect inhomogeneities in the structure and in the dynamics of the nanoscale point contact. The first reversible jump (E $\rightarrow$ F $\rightarrow$ E) causes a change of the relative magnitude of the backscattered electron flux of approximately 0.11% and the second one (A $\rightarrow$ C $\rightarrow$ A) leads to a relative change in the current of about 0.66%. These changes of the signals with respect to the axis may be due to the strong displacements of the atoms in the z-direction in both reversible relaxations.

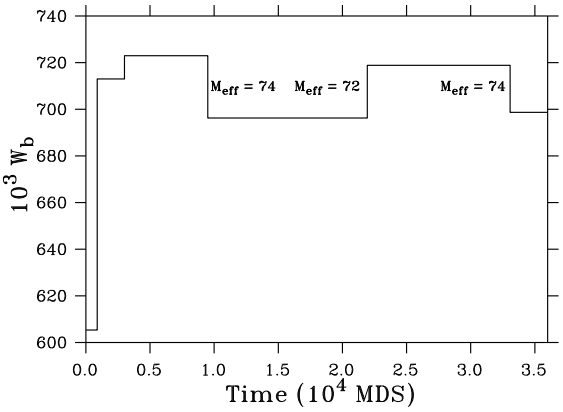

Figure 5. The fluctuator behaviour of a configuration with $N = 500$ atoms, which partially crystallized at a temperature $T = 0.05T_g$. The last three jumps with effective masses $M_{\rm eff} = 74m, 72m, 74m$ have jump lengths $\Delta R = 7.75\sigma, 6.83\sigma$ and 6.53σ, respectively. These relaxations are strongly correlated with $c_{RR'} = 0.958, 0.996$. W_b is plotted against time in units of MDS.

Additionally we calculated the backscattered current also for a partially crystallized defect structure of $N = 500$ atoms. After heating to $0.05T_g$ the configuration begins to crystallize. During the observation time the sample relaxes to another defect configuration. The initial relaxation is accompanied by a large drop in energy ($\Delta E = 30.28\epsilon$) while the following jumps lead to minima with similar energies ($\Delta E < 10^{-7}\epsilon$); in the last relaxation the system jumps to a minimum with slightly higher energy than the one preceding it ($\Delta E = 0.006\,70\epsilon$). The corresponding jump length is $\Delta R = 13.70\sigma$ for the initial relaxation. For the three following jumps ($\Delta R = 5.23\sigma, 7.75\sigma, 6.83\sigma$) with small energy changes we find effective masses $M_{\rm eff} = 68m, 74m, 72m$, respectively. For the last jump the

effective mass is about $74m$ and the jump length is about 6.53σ. The jumps following the initial decrease in energy are strongly correlated, i.e. mostly the same atoms are involved. Figure 5 shows the results for the calculations of the backscattering flow W_b plotted versus the observation time. The amplitude of the fluctuations after the initial step is about 3%.

So far we have considered monatomic metallic glasses, where due to crystallization effects long observation times are not accessible. Compared to the soft-sphere glasses the models for selenium are more stable, and longer observation times are possible without an appreciable drop in potential energy. Therefore, we also report results for the backscattered electron flux, normalized with respect to the incident flow, for a selenium glass. Although selenium is not a metal, the complex structure comprising chains and rings may be a good model for atomic entities forming the 'fluctuators'.

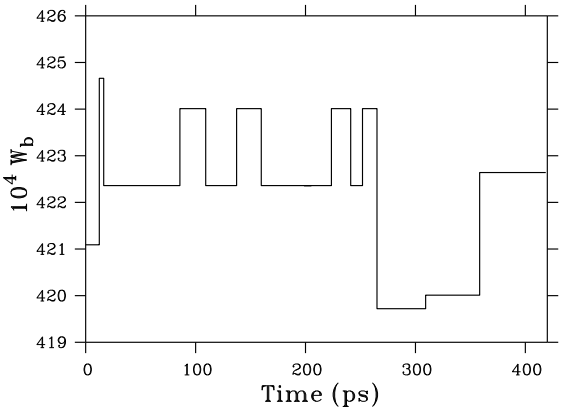

Figure 6. The fluctuator behaviour of a configuration with $N = 750$ Se atoms, at a temperature $T = 0.04T_g$. During the time range $t = 15$–260 ps the glass switches between two configurations. The effective mass of the reversible jumps is $M_{\text{eff}} \approx 10$ and the jump length $\Delta R \approx 0.5$ Å. The signal of the fluctuation is about 0.42% of the total contribution. W_b is plotted against time in units of ps.

The interaction of the Se atoms is described by a short-range three-body potential [30]. The glasses are produced by quenching corresponding liquids with quench rates of $\dot{T} = 10^{12}$–10^{14} K s^{-1} and pressures up to 10 GPa [23]. Note that if the quenching were too rapid, density fluctuations of the liquid could be frozen in. One possible way to avoid the formation of resulting micropores is to apply lower quench rates and/or pressure. The glasses are heated to temperatures of about $0.30T_g$ and then observed for approximately 0.5 ns at every temperature (this corresponds to roughly 3400 high-frequency vibrations). In figure 6 we plot the backscattered flow W_b versus time for a glass of $N = 750$ atoms at $T \approx 0.04T_g$. One can clearly observe a telegraph signal caused by a reversible jump occurring four times during the observation period. Its effective mass is $M_{\text{eff}} = 10$ and its total jump length $\Delta R = 0.5$ Å. The amplitude of the fluctuation is about 0.42% of the total interference contribution to the backflow.

4. Discussion and conclusions

We calculated the conductance fluctuations via the standard Landauer formula from the change of backscattering by the atoms comprising the junction. For the small junctions considered here electron scattering can be treated ballistically in the weak-scattering limit.

In geometries where multiple scattering is important, different methods have to be used. Todorov and Sutton, and Bratkovsky *et al* combine a molecular dynamics simulation with a T-matrix approach within the tight-binding approximation to calculate the conductance through atomic-scale metallic contacts during pull-off [31–33]. In agreement with experiment, they observe conductance jumps due to atomic rearrangements in the tip.

We want to point out that our approach is not suitable for reproducing the limiting case where the point contact merges into the crystalline structure. In this limit the conductance is no longer dominated by the scattering of the atoms in the junctions and the aperture.

Let us now consider the characteristic magnitude of the non-stationary current fluctuations. As seen from equation (4), one can discriminate between two terms:

(i) the 'classical' backscattering related to the diagonal terms in the sum of equation (4) which is independent of the coordinates of the scatterers and thus is not sensitive to relaxations; and

(ii) the interference contribution due to the $N(N-1)$ non-diagonal terms proportional to cosines and depending on the positions of the atoms.

For a given mode $\boldsymbol{k}$ and for a given position $\boldsymbol{r}$ in the detector plane, the standard deviation of the interference term is $\sim\sqrt{N(N-1)} \sim N$. However, additional averaging over the $\sim N^{2/3}$ different modes and over the different positions of $\boldsymbol{r}$ reduces the standard deviation to $N/(N^{2/3})^{1/2}(N^{2/3})^{1/2} = N^{1/3}$. Here positions separated by distances larger than $\sim 1/k$ are to be considered as independent, as regards the interference, giving in our units about $N^{2/3}$ independent positions. Therefore, the total standard deviation of the interference contribution due to a displacement of all scatterers is smaller than the average backscattered flow by about a factor of $N/N^{1/3} = N^{2/3}$. If one considers the current transport according to the concept of 'quantum channels', where in the weak-scattering limit each elementary cell in the point contact orifice roughly corresponds to one channel, the standard deviation of the interference contribution is of the order of the contribution of one channel, in agreement with the picture of universal conductance fluctuations (see, e.g., reference [34]).

For a shift of a single scatterer (affecting N terms in the summation over i, j in equation (4)) the effect is expected to be reduced by $N^{1/2}$, while for an uncorrelated jump of M atoms the expected effect is $\sim M^{1/2}/N^{2/3}N^{1/2} \sim M^{1/2}N^{-7/6}$ (normalized with respect to the average backflow current). Thus a jump of about 15 atoms out of 500 should give a fluctuation of relative magnitude ~ 0.003.

As seen, the order of magnitude of the experimental results is in agreement with this estimate. Some larger effects shown in figure 5 can be related to the fact that in fact the jumps cannot be considered as incoherent shifts of M atoms; the coherency of the atomic motion can increase the observed effect. Qualitatively, the results show the decrease of the relative fluctuation with increasing N and with decreasing M. The magnitude of the fluctuations gives information about the size of the relaxing region and about the character of the motion.

The occurrence rate of the fluctuations is many orders of magnitude smaller than characteristic vibrational frequencies of the structure and thus we are obviously dealing with slowly relaxing degrees of freedom. However, for the simulated structures the rate is still much larger than a typical frequency for the telegraph noise observed in real experiments [1, 2]. The reason is again the instability of the structures studied with respect to crystallization which simply prevents long observation times, which is in particular related to the small sizes of the systems and to the role of the periodic boundary conditions. In real systems, relaxations would be slowed down due to strains exerted by the embedding material. From our point of view, the simulations give a good model for the slowly relaxing multi-

stable entities in real structures. The structures in real point contacts will be somewhere in between the amorphous and partially crystalline state. In this respect we would especially like to emphasize that the multistable defects were also demonstrated for the simulated crystalline defect structure of figure 5.

The simulated current fluctuations exhibit a rather complex time behaviour. The complex behaviour shown in figure 4 results from jumps connecting eight different configurations of nearly equal energy. Since the initial and final configurations are identical, all jumps are reversible. Some jumps might trigger each other, while others will occur randomly. For example, after 42 000 MDS a jump followed immediately by the return jumps occurs; 15 000 MDS later, the same jump is followed by two different jumps before returning to the start configuration. In fact, the simulated picture resembles the one observed for real metallic contacts [2] at high enough temperatures referred to as 'fluctuator melting'. We would like to emphasize that the slowing down of relaxations with temperature prevented us from making studies of the extremely low temperatures where simpler two-state telegraph signals are expected. We want to emphasize, however, that the temperatures of our simulations are still far below the glass-transition and melting temperatures. We see a similarity to real experiments [2] where 'fluctuator melting' was observed at temperatures of about 100 K, i.e. far below the melting temperature of the metal.

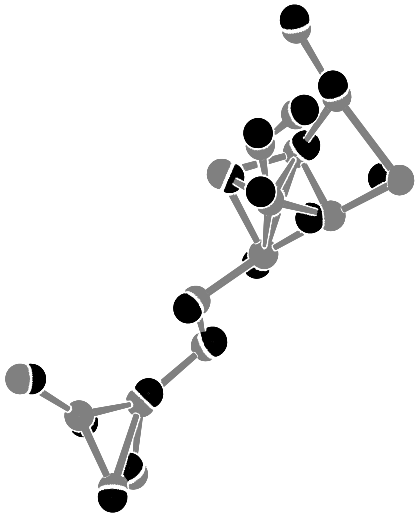

Figure 7. The reversible relaxation at $T = 0.1T_g$ observed in a glass with $N = 5488$ atoms. Full spheres depict the initial positions of the atoms; shaded spheres depict the atomic positions after the relaxation. Shown are all atoms with a displacement of more than 0.4 of the maximal contribution to this relaxation. The effective mass of this relaxation is $M_{\text{eff}} = 18m$ and the total jump length is $\Delta R = 1.22\sigma$. The largest contribution of a single atom to this jump is $\Delta R_{\text{max}} = 0.29\sigma$. The backscattering contribution of this jump is shown in figure 4.

Our simulations show that typically the 'fluctuators' involve large groups of atoms comprising up to 100 particles arranged mainly along some preferential direction. In figure 7 we show such a fluctuator identified by the of MD simulations for the current noise shown in figure 4. The atoms contributing strongly to the relaxation are shown with their respective initial and final positions marked as full and shaded circles. The structure formed by the particles resembles a chain with side branches. Note that the displacement of the atoms from the initial minimum to the second one is nearly a one-directional displacement (along the

chain). This fluctuator corresponds in figure 4 to the pronounced reversible relaxation after 42 000 MDS with an effective mass $M_{\text{eff}} = 18m$ and a total displacement $\Delta R = 1.22\sigma$.

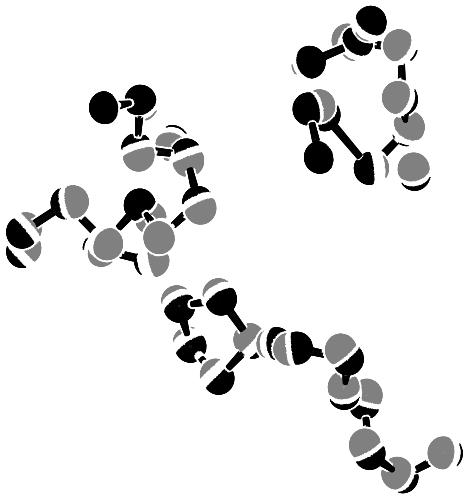

Figure 8. The reversible relaxation at $T = 0.04T_g$ observed in a Se glass with $N = 750$ atoms. Full spheres depict the initial positions of the atoms; shaded spheres depict the atomic positions after the relaxation. Shown are all atoms with a displacement of more than 0.2 of the maximal contribution to this relaxation. The maximal contribution to this relaxation is $\Delta R_{\max} = 0.44$ Å. The backscattering contribution of this jump is shown in figure 6.

Multistable configurations are more easily formed in the more complex Se structure. To some extent this hints towards a possible role of complex defects in the formation of fluctuators. In figure 8 we show the atoms which strongly participate in the telegraph noise shown in figure 6 for $t < 250$ ps. The complexity of the relaxation is reflected by the fact that the atoms of two regions of the system strongly participate in the jump. One of the structures of the relaxing entity is nearly one dimensional and the atoms comprising this structure move cooperatively along this preferential direction. In particular, one can speculate on the apparent similarity between the helical structure in Se and the structure near the core of a screw dislocation. In this respect we would like to mention the experimental studies [35] where the observed $1/f$ noise was shown to originate from atomic motion near dislocation cores.

One notes that the picture of the current behaviour is more complex than simple fluctuations which average out over long enough timescales which are not accessible in MD simulations. We observe a number of relaxations and related current fluctuations with different relaxation times. The time window of our simulation is too narrow to determine whether these fluctuations obey a $1/f$ law in the large-ensemble or long-time limits.

To conclude, in the framework of a simple model we have carried out a first simulation of multistable current noise in disordered contacts. The slowly relaxing modes responsible for the noise are visualized. The dependence of the magnitude of the noise on the size and structure of the modes was studied. In particular, the role of coherent atomic motion was emphasized. An important feature is a drastic change in the fluctuator dynamics (a transition to a complex multistable character of the fluctuations) at temperatures of about a tenth of the melting temperature of the sample; this behaviour agrees with 'fluctuators melting' reported for real metallic point contacts [2].

Acknowledgments

We are indebted to H R Schober and V L Gurevich for reading the manuscript and for many valuable remarks and discussions. One of us (VIK) acknowledges the hospitality of the Institut für Festkörperforschung of the Forschungszentrum Jülich and the financial support given by the German Ministry of Technology under the Russian–German scientific cooperation agreement. One of us (CO) gratefully acknowledges funding by the Deutsche Forschungsgemeinschaft through the Sonderforschungsbereich 408.

References

[1] Rogers C T and Buhrman R A 1984 *Phys. Rev. Lett.* **53** 1272
[2] Ralls K S and Buhrman R A 1988 *Phys. Rev. Lett.* **60** 2434
[3] Kogan A M and Nagaev K E 1984 *Solid State Commun.* **49** 387
[4] Ludviksson A, Kree R and Schmid A 1984 *Phys. Rev. Lett.* **52** 950
[5] Kozub V I 1984 *Sov. Phys.–JETP* **86** 1303
[6] Kozub V I 1984 *Sov. Phys.–Solid State* **26** 1851
[7] Kozub V I 1984 *Sov. Phys.–JETP* **60** 818
[8] Galperin Yu M, Karpov V G and Kozub V I 1989 *Adv. Phys.* **38** 669
[9] Muller C J, van Ruitenbeck J M and de Jongh L J 1992 *Phys. Rev. Lett.* **69** 140
[10] Kozub V I and Rudin A M 1993 *Phys. Rev.* B **47** 13 737
[11] Laird B B and Schober H R 1991 *Phys. Rev. Lett.* **66** 636
Schober H R and Laird B B 1991 *Phys. Rev.* B **44** 6746
[12] Schober H R, Oligschleger C and Laird B B 1993 *J. Non-Cryst. Solids* **156–158** 965
Schober H R and Oligschleger C 1996 *Phys. Rev.* B **53** 11 469
[13] Pelz J and Clarke J 1987 *Phys. Rev.* B **36** 4479
[14] Martin J W 1971 *Phil. Mag.* **24** 555
[15] Galperin Yu M and Kozub V I 1991 *Sov. Phys.–JETP* **73** 179
[16] Beenakker C W J and van Houten H 1991 Quantum transport in semiconductor nanostructures *Solid State Physics* vol 44 (New York: Academic)
[17] Glazman L I, Lesovik G B, Khmel'nitskii D E and Shekhter R I 1988 *JETP Lett.* **48** 218
[18] Kirczenow G 1988 *Solid State Commun.* **68** 715
[19] Kozub V I, Caro J and Holweg P A M 1994 *Phys. Rev.* B **50** 15 126
[20] Grincwajg A, Edwards G and Ferry D K 1996 *Physica* B **227** 54
[21] Born M and Wolf E 1959 *Principles of Optics: Electromagnetic Theory of Propagation and Diffraction of Light* (London: Pergamon) pp 374
[22] Landau L D and Lifshitz E M 1972 *Quantum Mechanics* (Oxford: Pergamon)
[23] Oligschleger C and Schober H R 1993 *Physica* A **201** 391
[24] Oligschleger C and Schober H R 1995 *Solid State Commun.* **93** 1031
[25] Hoover W G, Gray S G and Johnson K W 1971 *J. Chem. Phys.* **55** 1128
[26] Fletcher R and Reeves C M 1964 *Comput. J.* **7** 149
[27] Oligschleger C and Schober H R 1998 submitted
[28] Schober H R, Gaukel C and Oligschleger C 1997 *Defect Diffusion Forum* **143–147** 723
[29] Ehrhart P, Robrock K H and Schober H R 1986 *Physics of Radiation Effects in Crystals* ed R A Jonson and A N Orlov (Amsterdam: North-Holland) p 3
[30] Oligschleger C, Jones R O, Reimann S M and Schober H R 1996 *Phys. Rev.* B **53** 6165
[31] Todorov T N and Sutton A P 1993 *Phys. Rev. Lett.* **70** 2138
[32] Bratkovsky A M, Sutton A P and Todorov T N 1995 *Phys. Rev.* B **52** 5036
[33] Todorov T N and Sutton A P 1993 *Phys. Rev.* B **54** R14 234
[34] Feng S, Lee P A and Stone A D 1986 *Phys. Rev. Lett.* **56** 1960
[35] Ochs E, von Homberg M J C, Alkemade P F A, Armbruster K, Seeger A, Stoll H and Verbruggen A H 1997 *Noise in Physical Systems and* $1/f$ *Fluctuations; Proc. 14th Int. Conf.* ed C Claeys and E Simoen (Singapore: World Scientific) p 415